2020

Dynamic analysis of fault slips and their influence on coal mine rib stability

Jan Nemcik
University of Wollongong

Gaetano Venticinque
SCT Operations Pty Ltd

Libin Gong
Czech Academy of Science

DYNAMIC ANALYSIS OF FAULT SLIPS AND THEIR INFLUENCE ON COAL MINE RIB STABILITY

Jan Nemcik[1], Gaetano Venticinque[2] and Libin Gong[3]

ABSTRACT: Historical data indicate that in deep coal mines the presence of faults in close proximity to excavations affect the frequency of coal bursts. A number of researchers have attempted to correlate the fault geometries to the frequency and severity of coal bursts but dynamic numerical modelling has not been used to show how faults can affect coal ejection from the rib side. The dynamic numerical analysis presented here show how different orientations of fault slips may affect coal bursts. To prove the concept, 89 cases of slipping fault geometries were modelled using the FLAC^{3D} software and their effect on rib stability investigated. The results indicate that there is a simple and logical correlation between the fault location, its slip velocity and the ejection of the yielded coal rib side. The seismic compressive wave generates rock/coal mass velocities that directly impact the rib side. If the coal rib is relatively disturbed and loose, these velocities can cause its ejection into the excavation. The slip direction typically impacts one side of the mine roadway only. A 1 m thick loose coal block attached to the 3 m high rib side in mine roadway was ejected at speeds ranging from 2.5 to 5 m/s depending on the fault location, its orientation and the maximum fault slip velocity modelled at 4 m/s.

INTRODUCTION

Many researchers participated in investigating the origins and causes of rock/coal bursts with various success including Bräuner (1994), Brown, S. (1998), Brune (1993), Chengguo (2017), Dou (2016), Hebblewhite (2017), Mark (2014), Moodie (2011), Muller (1991), among many others. The lengthy principles and mechanisms of fault and seismic behaviour in these investigations are not included here, instead this description is focused directly on the principles behind the investigations and the modelled results as reported in the ACARP C26054 project (Nemcik et al. 2019).

The seismic waves in rock generate a 'back and forward' sinusoidal motion of the individual rock particles at relatively low speeds, usually several m/s. The maximum velocity of this particle movement is also known as the peak particle velocity (PPV) caused by the seismic waves (Saharan, 2004). This movement transfers the energy momentum along the rock mass at very fast speeds of up to several km/s. PPV is widely used as a threshold for damage to the rock mass (Brinkmann, 1987) and can determine the magnitude of damage caused by seismic events. This mechanism is similar to the Newton's cradle motion. When rock/coal motion approaches the unconfined rib side, it may rip apart the already weakened coal rib and 'knock' the failed/loose coal out into the excavation. This is depicted in the top layer in Figure 1(e) where the detached last ball (mass) is knocked out and carry the accumulated energy with it. No wave reflection occurs. On the other hand, if the edge mass (shown in the bottom layer) is firm/attached, the seismic wave is reflected and no rib mass is damaged or ejected Figure 1 (e) and (f). Another view of the same burst mechanism is schematically depicted in Figure 2 where

[1] *Honorary Senior Fellow, University of Wollongong. Email: jnemcik@uow.edu.au Tel: +61 2 4221 4492*

[2] *Senior Geotechnical Engineer, SCT Operations Pty Ltd, Email: gventicinque@sct.gs*

[3] *Researcher, The Czech Academy of Sciences, Institute of Geonics, libin.gong@ugn.cas.cz, Tel: +420 596 979 701*

the mass momentum travels through the laterally compressed seam knocking the loose rib mass into the excavation. Typically, the yielded coal located close to the roadway is broken and relatively loose with lower confining stress and therefore it can be easily knocked out of the rib.

There are many types of stored potential energy that can contribute to the coal burst. Examples of these include: slip of highly loaded fault plane, geologically weakened coal-rock interfaces, high additional loads due to nearby mining, among others. For the rock burst to occur, a dynamic event such as a fault slip is needed to generate the seismic waves and supply enough energy to dislodge the already stressed or non-existent bonds between the coal seam and the roof/floor rock interfaces.

Two sources of the seismic energy can be in play simultaneously consisting of the propagating seismic disturbance from the fault slip together with the release of stored energy in the compressed coal seam. The example of generated seismic waves is depicted in Figure 3. However, the fault slips may generate sufficient amount of seismic energy to produce a coal burst on its own.

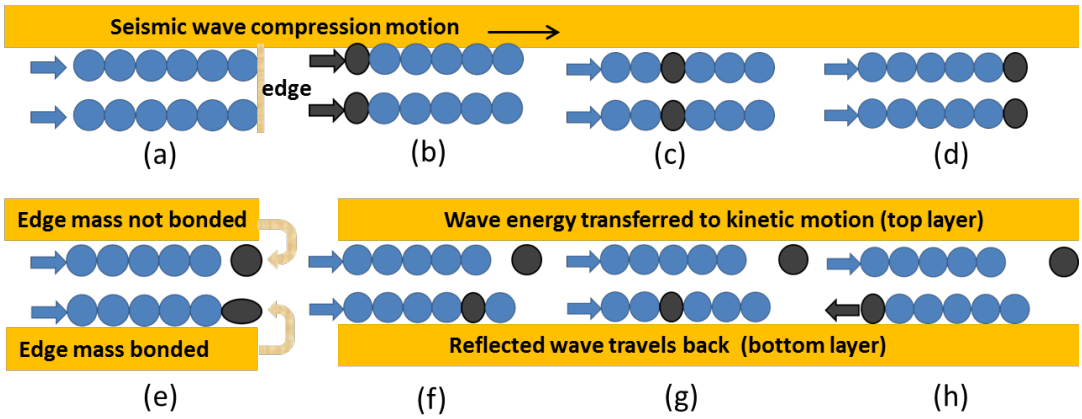

Figure 1: Schematic of seismic compression wave in rock, (a) and (b) Seismic wave hits and compresses the rock mass, (c) and (d) Compression in rock mass is travelling at sonic speed, (e) in the top layer, the disconnected rock mass flies out into the empty space - no reflection occurs. In the bottom layer the connected mass stretches and rebunds back impacting the mass on the left side – reflection occurs, (f), (g) and (h) in the bottom layer the reflected seismic wave propagaes back to the left at the sonic speed.

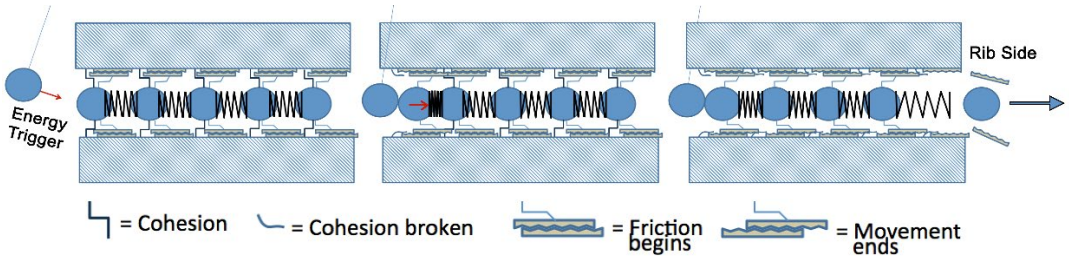

Figure 2: Modified Newtons Cradle as an analogy of the rock burst where the yielded coal is ejected from the rib

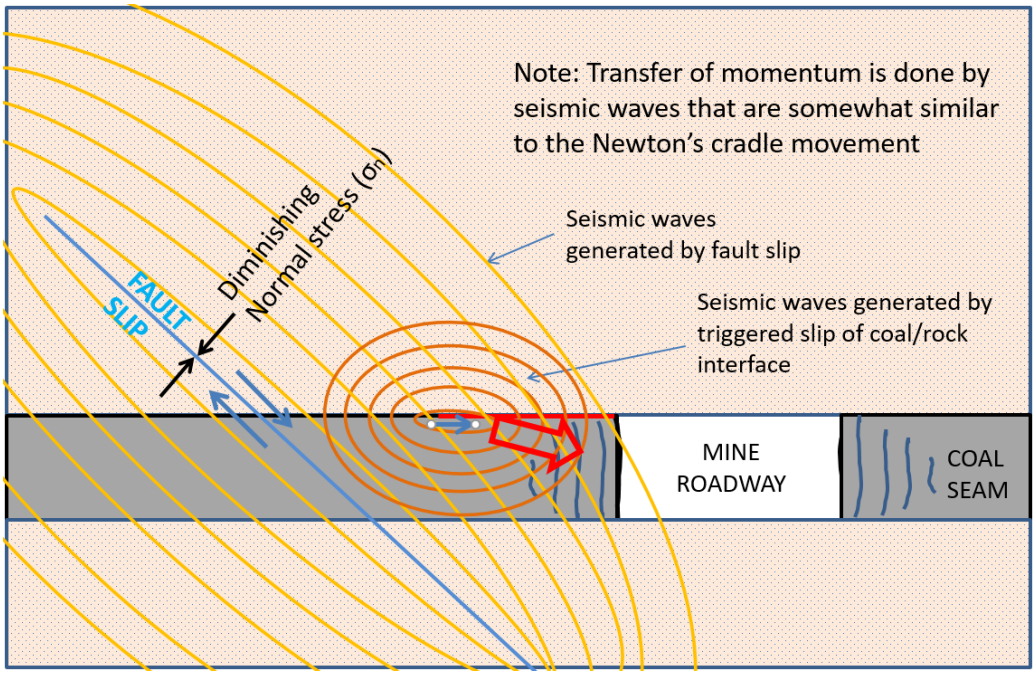

Figure 3: Fault slip mechanism, generation of seismic waves and their impact on coal

The exact mechanism of the fault slip is still not very well known. Many researchers carried out back analysis of seismic events trying to estimate fault properties and their influence on PPV in the near field. Their research indicates that various fault surface properties appear to influence the seismic parameters (Sainoki and Mitri, 2016). From the far-field S-wave pulses in a deep underground mine McGarr (1991) estimated fault slip velocity rates ranging from 1 to 5 m/s.

The purpose of this dynamic numerical model presented here is to investigate the overall rib behaviour when the nearby fault slip occurs. For that the fault slip value equal to 4 m/s was chosen. To evaluate the influence of this particular fault slip on coal rib stability, an average seismic energy impacting the rib side was calculated for 1 m length of roadway. This was derived from the kinetic momentum of an ejected coal block that was loosely attached to the coal rib at the studied locations. These calculations and geometries aimed at producing basic results to prove that this method could be used to flag dangers of coal burst occurrence for certain fault orientations that may exist near excavations. Many models with various fault orientations produced data shown in Table 1. To avoid any complications that may occur with yielded zones, elastic models were set up to carry out the sensitivity studies investigating the influence of fault orientation, distance from the excavation, direction of probable fault slip and side/location within the excavation that may experience the coal burst. Once the location of the fault zone is known, the mine excavation side where rib ejection may occur can be estimated. This makes this research very valuable for safety in coal mines as workers may be able to keep from the harm's way while mining through certain zones of fault influence.

Table 1: Model Strata Properties

Mechanical properties	Sandstone	Coal
Density	2500 kg/m^3	1400 kg/m^3
Bulk modulus	10.67 GPa	3.33 GPa
Shear modulus	6.4 GPa	1.11 GPa

DYNAMIC MODEL SETUP IN FLAC^{3D}

The constructed model was 80 m wide (perpendicular to the mined roadway), 80 m high and 40 m thick as shown in Figure 4. To examine the first 44 fault geometries with the fault plane aligned with the mine roadway, the 5 m wide mine roadway was excavated through the model centre in a 3 m thick coal seam. A continuous 2.9 m high and 1 m thick coal block was attached to the rib side in the mine roadway to measure kinetic momentum of seismic waves delivered to the rib side. For the remaining 45 fault models a shorter mine roadway was excavated to the centre of the model and a 1 m thick, 2.9 m high and 2 m long coal block was attached to the rib side adjacent to the roadway face. Elastic properties of the strata were chosen to enable measurements of the maximum possible kinetic energy transfer through the rock and coal seam without complications of the yielded zones. Typical sandstone rock and coal properties were assigned to the roof, floor and the coal seam as specified in Table 1.

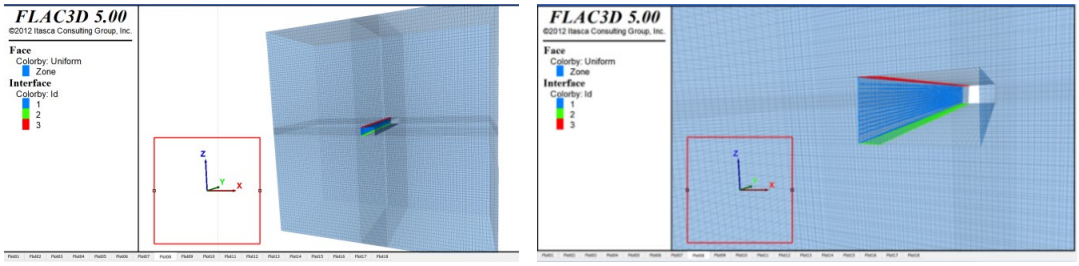

Figure 4: Model geometry showing excavated mine roadway

Each model was run until static equilibrium was achieved. A simple one way dynamic fault slip was artificially modelled by assigning variable slip velocities along each fault using the decay equation:

$$y(t) = A^{-\lambda ct}\cos(2\pi ct + \varphi) \quad (1)$$

Where A is wave amplitude (18.4 m/s – not the actual fault slip velocity produced)
λ is constant (10)
φ is phase (90°)
c is constant (7) and
t is time (between 0 to 0.07s)

The chosen equation constants produced the maximum fault slip velocity of 4 m/s that occurred at time t = 0.013 seconds after the slip began and subsequently decayed to zero at approximately 0.07 seconds, producing total slip displacement of 119 mm. The graph of fault slip vs time (from Eq1) is shown in Figure 4(a). These values were estimated from previous dynamic numerical models by studying mining induced fault slips in metalliferous mines (Sainoki, 2014). The first rib dynamic impact was produced by the rapidly increasing velocities within the short time of 0.013 seconds as the kinetic momentum carrying waves spread through the strata at sonic speeds. Subsequent decay velocities during the fault slip did not seem to significantly influence the mine roadway stability.

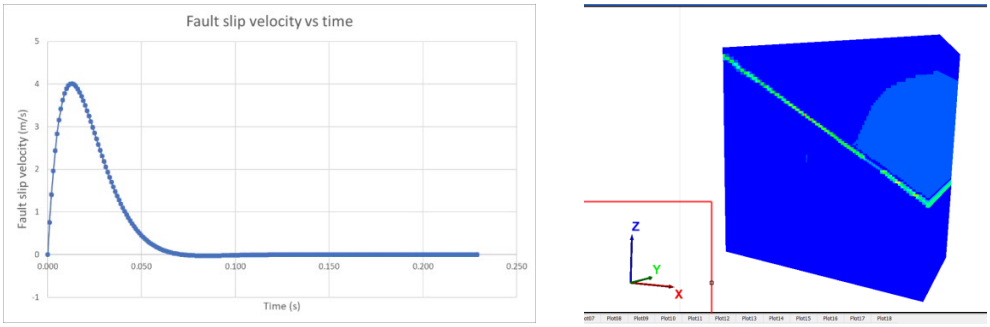

(a) (b)

Figure 5: (a) Fault slip velocity versus time using Eq (1), (b) geometry of one of the slipping faults

MODELLED FAULT SLIP FAILURE AT VARIOUS FAULT ORIENTATIONS AND THEIR INFLUENCE ON ROADWAY RIB STABILITY

Horizontal faults parallel to the seam were modelled 2 m, 5 m, 10 m, 15 m, 20 m and 30 m below the seam floor. This was repeated in the roof with the same distances above the seam roof. These faults were subsequently rotated from 0° to dips of 15°, 30°, 45°, and 60° through the fault rotation point which was located below the roadway centre and above in the roof at the same distances from the seam roof and the floor. Additional 45 runs of the vertical fault at various distances and bearings ahead of the roadway face were also trialled.

The fault slips were arranged so that the impact from the slip was oriented towards the rib side where the attached coal block was placed. As the fault slipped, it produced seismic waves carrying the kinetic energy (momentum) that travelled towards the rib. To measure the rib side impact energies, a continuous 1 m wide coal block was attached to the rib side in the first 44 modelled faults. This block was used to simulate the yielded and only slightly confined coal mass typically found in the fractured coal rib. This block was important to measure the rib momentum more precisely as the rock mass in FLAC model is continuous and the model zones cannot normally part from the rib. A section of coal was excavated, interfaces were assigned to its surface, and the block placed in the roadway touching the rib. The model was first brought to a static equilibrium and then the fault slip was initiated. The seismic waves impacted the block, ejecting it from the rib side. This mechanism provided the controlled way to measure the impact velocities generated by the seismic waves at the coal rib.The fault slip induced seismic waves quickly spread through the surrounding strata impacting the roadway rib. Note that the slip direction typically impacts only one side of the roadway. This is shown in Figure 6(a) where the grid velocities initiated by the seismic wave are spreading away from the slip boundary in the direction of the final block ejection. Note that the fault slip directions can be determined from the ground stress.

After the seismic waves dissipated through the surrounding strata, the seismic momentum, locked inside the block, propelled the block at velocities above 4 m/s shown in Figure 6(b). For non-elastic conditions smaller dynamic impacts may occur. Further work is needed to incorporate fully yielded models, faults affected by stress relief due to excavation, and use fault slip data measurements if available.

For the vertical faults numbered 45 to 89, the mine roadway was excavated half way into the model centre and faults inserted in front of the roadway face. A coal block 1 m thick, 2.9 m high and 2 m long was attached to the roadway rib side adjacent to the roadway face. An example of this block ejection velocity of 4 m/s after the fault slip is shown in Figure 7.

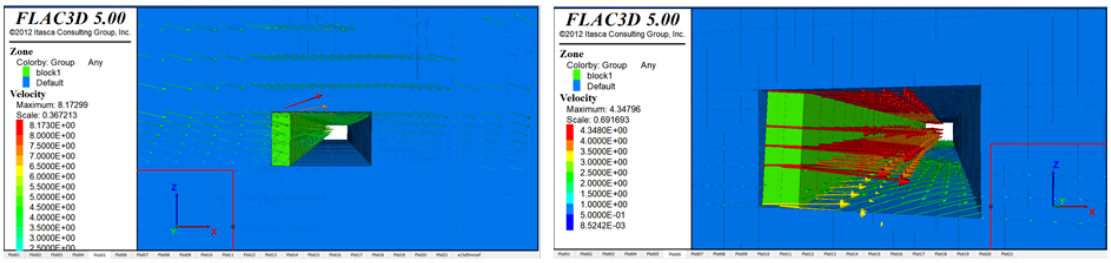

(a) **(b)**

Figure 6: (a) Development of velocities induced by slipping fault (15° dip) 5 m above the roadway at time of 0.012 seconds after fault slip began, (b) View inside the mine roadway showing the coal block ejection at an average velocity above 4 m/s at time of 0.07 seconds.

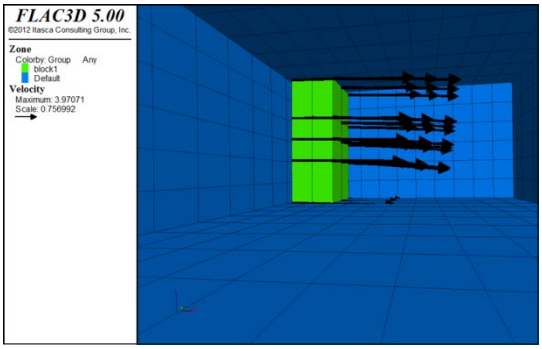

Figure 7: View inside of the excavated mine roadway showing the coal block and its ejection away from the rib side

CALCULATIONS OF SEISMIC IMPACT AT THE RIB SIDE

The simplified method chosen to enable calculations of the dynamic impact produced by seismic momentum reaching the mine roadway rib is defined by the kinetic momentum delivered to the rib per m of roadway perpendicular to the rib (first impact only) $P = mv$, *where P is the kinetic momentum (kgm/s), m is ejected mass (kg) and v is the mass velocity (m/s).*

The kinetic energy delivered to the rib per m of roadway perpendicular to the rib (at first impact only) is: $E = \frac{1}{2}mv^2$ *where E is the kinetic energy (Nm), m is ejected mass (kg) and v is the mass velocity (m/s).*

The first 44 models examined influence of faults with their plane aligned parallel to the roadway mining direction at various distances above and below the seam and dips varying from horizontal to 60° degrees. The vertical faults numbered from 45 to 89 were at various distances ahead of the roadway face and various orientations from 60° to -60°, 0° being parallel to the roadway face. The calculations of coal block ejection velocities, kinetic momentum and kinetic energy were performed for each fault slip at various locations and orientations and are summarised in Table 2.

Table 2: Modelled fault geometry, block ejection velocities and rib impact energy due to fault slip

Fault No	Strike (°)	Dip (°)	Fault Distance from seam (m)	Block Ejection average velocity (m/s)	Block Momentum (mv)	Energy impacting the rib (kNm)
1	Parallel to seam	0°	20m Roof	4.1	17.1	35.8
2	Parallel to seam	0°	15m Roof	4.3	17.5	37.5
3	Parallel to seam	0°	10m Roof	4.4	17.9	39.3
4	Parallel to seam	0°	5m Roof	4.3	17.5	37.5
5	Parallel to seam	0°	2m Roof	3.5	14.2	24.9
6	Parallel to seam	0°	2m Floor	3.9	15.8	30.9
7	Parallel to seam	0°	5m Floor	4.5	18.3	41.1
8	Parallel to mining	0°	10m Floor	4.6	18.7	43.0
9	Parallel to mining	0°	15m Floor	4.6	18.7	43.0
10	Parallel to mining	0°	20m Floor	4.5	18.3	41.1
11	Parallel to mining	15°	20m Roof	4.1	16.6	34.1
12	Parallel to mining	15°	15m Roof	4.3	17.5	37.5
13	Parallel to mining	15°	10m Roof	4.3	17.5	37.5
14	Parallel to mining	15°	5m Roof	4.4	17.9	39.3
15	Parallel to mining	15°	2m Roof	4.3	17.5	37.5
16	Parallel to mining	15°	2m Floor	4.3	17.5	37.5
17	Parallel to mining	15°	5m Floor	4.6	18.7	43.0
18	Parallel to mining	15°	10m Floor	4.4	17.9	39.3
19	Parallel to mining	15°	15m Floor	4.7	19.1	44.8
20	Parallel to mining	15°	20m Floor	4.2	17.1	35.8
21	Parallel to mining	30°	20m Roof	4.0	16.2	32.5
22	Parallel to mining	30°	15m Roof	4.5	18.3	41.1
23	Parallel to mining	30°	10m Roof	4.4	17.9	39.3
24	Parallel to mining	30°	5m Roof	4.2	17.1	35.8
25	Parallel to mining	30°	2m Roof	4.2	17.1	35.8
26	Parallel to mining	30°	2m Floor	4.2	17.1	35.8
27	Parallel to mining	30°	5m Floor	4.2	17.1	35.8
28	Parallel to mining	30°	10m Floor	4.3	17.5	37.5
29	Parallel to mining	30°	15m Floor	4.3	17.5	37.5
30	Parallel to mining	30°	20m Floor	4.2	17.1	35.8
31	Parallel to mining	45°	15m Roof	4.2	17.1	35.8
32	Parallel to mining	45°	10m Roof	4.4	17.9	39.3
33	Parallel to mining	45°	5m Roof	4.4	17.9	39.3
34	Parallel to mining	45°	2m Roof	4.4	17.9	39.3
35	Parallel to mining	45°	2m Floor	4.2	17.1	35.8
36	Parallel to mining	45°	5m Floor	4.2	17.1	35.8
37	Parallel to mining	45°	10m Floor	4.2	17.1	35.8
38	Parallel to mining	45°	15m Floor	4.2	17.1	35.8
39	Parallel to mining	60°	10m Roof	3.7	15.0	27.8
40	Parallel to mining	60°	5m Roof	3.6	14.6	26.3
41	Parallel to mining	60°	2m Roof	3.6	14.6	26.3
42	Parallel to mining	60°	2m Floor	3.0	12.2	18.3
43	Parallel to mining	60°	5m Floor	3.0	12.2	18.3
44	Parallel to mining	60°	10m Floor	2.8	11.4	15.9
45	0°	90°	3 m	4.9	19.9	48.7
46	0°	90°	6 m	4.9	19.9	48.7
47	0°	90°	9 m	4.9	19.9	48.7
48	0°	90°	12 m	5.0	20.3	50.8
49	0°	90°	15 m	5.0	20.3	50.8

Fault No	Strike (°)	Dip (°)	Fault Distance from seam (m)	Block Ejection average velocity (m/s)	Block Momentum (mv)	Energy impacting the rib (kNm)
50	15°	90°	3 m	4.9	19.9	48.7
51	15°	90°	6 m	4.9	19.9	48.7
52	15°	90°	9 m	4.9	19.9	48.7
53	15°	90°	12 m	5.0	20.3	50.8
54	15°	90°	15 m	4.8	19.5	46.8
55	30°	90°	3 m	4.5	18.3	41.1
56	30°	90°	6 m	4.5	18.3	41.1
57	30°	90°	9 m	4.6	18.7	43.0
58	30°	90°	12 m	4.6	18.7	43.0
59	30°	90°	15 m	4.4	17.9	39.3
60	45°	90°	3 m	3.8	15.4	29.3
61	45°	90°	6 m	3.8	15.4	29.3
62	45°	90°	9 m	3.8	15.4	29.3
63	45°	90°	12 m	3.8	15.4	29.3
64	45°	90°	15 m	3.8	15.4	29.3
65	60°	90°	3 m	2.7	11.0	14.8
66	60°	90°	6 m	2.7	11.0	14.8
67	60°	90°	9 m	2.8	11.4	15.9
68	60°	90°	12 m	2.8	11.4	15.9
69	60°	90°	15 m	2.8	11.4	15.9
70	-15°	90°	3 m	4.5	18.3	41.1
71	-15°	90°	6 m	4.6	18.7	43.0
72	-15°	90°	9 m	4.7	19.1	44.8
73	-15°	90°	12 m	4.6	18.7	43.0
74	-15°	90°	15 m	4.2	17.1	35.8
75	-30°	90°	3 m	4.2	17.1	35.8
76	-30°	90°	6 m	4.15	16.8	35.0
77	-30°	90°	9 m	4	16.2	32.5
78	-30°	90°	12 m	3.9	15.8	30.9
79	-30°	90°	15 m	3.8	15.4	29.3
80	-45°	90°	3 m	3.2	13.0	20.8
81	-45°	90°	6 m	3.2	13.0	20.8
82	-45°	90°	9 m	3.2	13.0	20.8
83	-45°	90°	12 m	3.2	13.0	20.8
84	-45°	90°	15 m	3.2	13.0	20.8
85	-60°	90°	3 m	2.5	10.2	12.7
86	-60°	90°	6 m	2.5	10.2	12.7
87	-60°	90°	9 m	2.5	10.2	12.7
88	-60°	90°	12 m	2.5	10.2	12.7
89	-60°	90°	15 m	2.5	10.2	12.7

The results summarised in Table 2 indicate that the faults with the same slip characteristics at close proximity to the excavation appear to produce similar block ejection velocities. These velocities seem to be similar to the maximum fault slip velocity. This is not surprising. When tracing the velocities surrounding the slipping fault, the 'particle' velocities that spread through either the rock or softer coal have similar maximum velocities and directions to the slipping fault if located nearby. This simplifies the understanding of basic seismic wave front propagation close to the faults.

It may be confusing to think of seismic waves as the 'extremely fast moving compressive or shear fronts'. It seems more logical to interpret the coal/rock matrix movement thinking about the 'peak particle velocities' (PPV) as vectors in rock that tend to disturb the unconfined

rock/coal integrity at the boundaries. The seismic wave conservation of kinetic momentum can also be better understood by imagining either large or small particle collisions in the wave front inside the rock matrix as shown earlier in Figure 1.

A minor refraction of seismic waves at the rock/coal seam interface (due to a slower speed of seismic waves in softer coal) produced velocity concentrations within the seam. Extra 45 dynamic runs were done modelling coal as rock to avoid the refraction of seismic waves. These tests indicated that there was a small decrease of 'rib coal block' ejection velocities in the 'rock seam' when compared to the 'coal seam'. This work indicates that the change in seismic velocity within soft coal seam has a magnifying effect on the rib impact magnitudes with increasing velocities ranging from being negligible to 20 %.

Observations of the coal block ejection indicated that the block side located closer to the slipping fault experienced dynamic impact sooner that the other block side. This caused block rotation and uneven ejection of these blocks. Furthermore, fault inclination produced inclined impact velocities to the rib, affecting block ejection trajectories further, causing the block to bounce up and down. This is illustrated in the examples shown in Figures 8 to 10. Note: To avoid the influence of friction along the roof and the floor, friction and cohesion properties along each interface were reduced to a bare minimum not to affect coal block velocities with time.

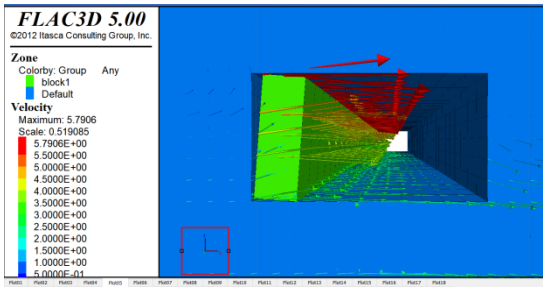

Figure 8: Block displacement and rotation after 0.07 seconds induced by horizontal fault slip 10 m above mine roadway

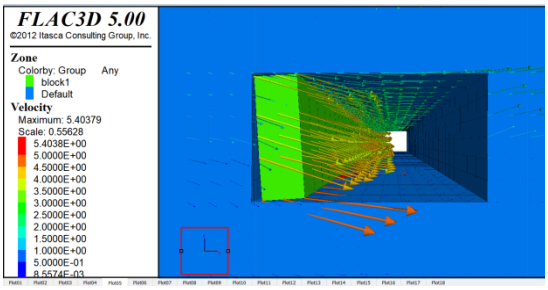

Figure 9: Block displacement and rotation after 0.07 seconds induced by horizontal fault slip 10m below mine roadway

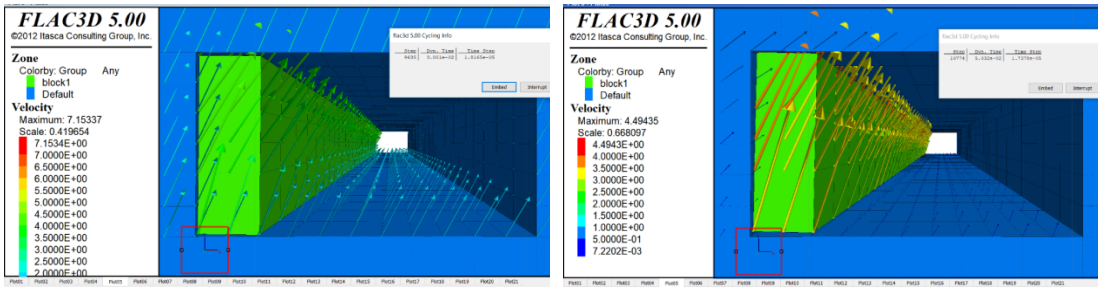

Figure 10: Block displacement induced by inclined (60° dip) fault slip 10m below mine roadway after (a) 0.024 seconds, (b) 0.05 seconds

SUMMARY

To study the fault induced seismic waves and its influence on coal bursts in 3-dimensions, 89 dynamic models of various fault-slip locations and directions were modelled using the FLAC^{3D}. The fault slip failure shows that this mechanism can generate sufficient amount of seismic energy to produce a coal burst on its own. Fault slip can typically occur as the progressive nearby excavations gradually relieve stress normal to the fault plane. The initial rib impact appears to be approximately proportional to the maximum velocity of fault slip. These fault slips release fast seismic waves that generate rock mass sinusoidal movement parallel to the fault

that can exceed several m/s. This study modelled many fault slips in various locations and orientations adjacent to the mine roadway showing fast ejections of the detached blocks into the roadway.

The results indicate the occurrence of coal burst to typically originate from one side of the roadway where the seismic waves directly impact the rib side. The models also show the tendency of seismic waves to concentrate inside the coal seam producing faster coal rib ejections. Once the location of the fault zone and the probable direction of fault slip is estimated, the side of the roadway where rib ejection is probable, can be predicted. This makes this research very valuable for safety in coal mines as workers may be able to keep from the harm's way by minimising their presence at the side where a potential rib impact may occur, while mining through certain zones of fault influence. It is suggested that more detailed dynamic numerical studies of the underground coal burst cases related to the presence of faults be undertaken.

REFERENCES

Bräuner, 1994, Rock bursts in coal mines and their prevention. Rotterdam:A.A. Balkema, ISBN: 978-1351418034

Brinkmann, 1987. Separating shock wave and gas expansion breakage mechanism

2nd International Symposium on Rock Fragmentation by Blasting (1987), pp. 6-15

Brown, S., 1998. Friction heating of faults, Stable sliding versus stick slip. Journal of Geophysical research Solid Earth, Vol. 103 (B4).pp 7413-7420.

Brune, J. N. Brown, S. and Johnson P.A., 1993. Rupture mechanism and interface separation in foam rubber models of earthquakes: a possible solution to the heat flow paradox and the paradox of large overthrusts. Science Direct,Tectonophysics, Vol. 218. Issues 1-3, pp 59-67.

Chengguo, Z., Canbulat, I., Tahmasebina, F. and Hebblewhite, B. 2017. Assessment of energy release mechanisms contributing to coal burst. International Journal of Mining Science and Technology, Vol. 27 (1), pp. 43-47.

Dou L., Mu Z., Li Z. Cao A. and Gong S., 2016. Research of rock burst monitoring, forecasting and prevention in coal mining in China. In proceedings of the 9th International Symposium on Green mining, Wollongong, Australia, University of Wollongong – Mining Engineering, pp. 382-391.

Hebblewhite, B. and Galvin, J., 2017. A review of the geomechanic s aspects of a double fatality coal burst at Austar Colliery in NWS, Australia in April 2014. International Journal of Mining Science and Technology, (Section A: Mining Industry), Vol. 100, pp. 22-30.

Itasca FLAC^{3D} Manual, 2015. Fast Lagrangian Analysis Continua – version 7.0 User Manual. Minneapolis, Minnesota, USA: Itasca Consulting Group.

Mark, C., (2014). Coal bursts in deep longwall mines of the United States. In: Proceedings of the 3rd Australasian Ground Control in Mining Conference (AusRock) Vol. (3), pp 33-40.

McGarr, A., 1991. Observations constraining near-source ground motion estimated from locally recorded seismograms. J. Geophys. Res., 96 (B10) (1991), pp. 16495-16508

Moodie, A. and Anderson, J., 2011. Geotechnical considerations of longwall top coal caving at Austar Coal Mine. In Proceedings of 30th Int. Conference on Ground Control in Mining, Morgantown, WV, USA, pp. 238-247.

Muller W., 1991. Numerical simulation of rock bursts. International Journal of Mining Science and Technology, Elsevier Science Publishers, Vol. 12 (1), pp. 27-42.

Nemcik J., Venticinque G. and Karekal S. (2019) Modelling of Dynamic Fracture Mechanisms for Improved Strata Control Design and Coal Burst Assessment, ACARP report C26054.

Saharan, M. (2004). Dynamic modelling of rock fracturing by destress blasting, Mining & Materials Engineering, McGill University, Montreal, QC, Canada (2004)

Sainoki, A. (2014). Dynamic modelling of mining-induced faultslip, PhD Thesis Department of Mining & Materials Engineering McGill University, Montreal, Canada

Sainoki, Atsushi; Mitri, Hani S. (2016). Back analysis of fault-slip in burst prone environment. Journal of Applied Geophysics. Volume 134, 159-171.

Venticinque, G. & Nemcik, J., 2017. Presentation at the 9th International Symposium on Green mining, Wollongong, Australia Green Mining Conference, Innovation Campus, University of Wollongong. Presentation only.